ACSNANO
www.acsnano.org
ARTICLE

# Reliability of Single Crystal Silver Nanowire-Based Systems: Stress Assisted Instabilities

Rajaprakash Ramachandramoorthy,[⊥,†,‡] Yanming Wang,[⊥,§] Amin Aghaei,[§] Gunther Richter,[∥] Wei Cai,[*,§] and Horacio D. Espinosa[*,†,‡]

[†]Department of Mechanical Engineering, Northwestern University, Evanston, Illinois 60208, United States
[‡]Theoretical and Applied Mechanics Program, Northwestern University, Northwestern University, Evanston, Illinois 60208-3111, United States
[§]Department of Mechanical Engineering, Stanford University, Stanford, California 94305-4040, United States
[∥]Max Planck Institute for Intelligent Systems, Heisenberg Street, Stuttgart 70569, Germany

*Supporting Information*

**ABSTRACT:** **Time-dependent mechanical characterization of nanowires is critical to understand their long-term reliability in applications, such as flexible-electronics and touch screens. It is also of great importance to develop a theoretical framework for experimentation and analysis on the mechanics of nanowires under time-dependent loading conditions, such as stress-relaxation and fatigue. Here, we combine *in situ* scanning electron microscope (SEM)/transmission electron microscope (TEM) tests with atomistic and phase-field simulations to understand the deformation mechanisms of single crystal silver nanowires held under constant strain. We observe that the nanowires initially undergo stress-relaxation, where the stress reduces with time and saturates after some time period. The stress-relaxation process occurs due to the formation of few dislocations and stacking faults. Remarkably, after a few hours the nanowires rupture suddenly. The reason for this abrupt failure of the nanowire was identified as stress-assisted diffusion, using phase-field simulations. Under a large applied strain, diffusion leads to the amplification of nanowire surface perturbation at long wavelengths and the nanowire fails at the stress-concentrated thin cross-sectional regions. An analytical analysis on the competition between the elastic energy and the surface energy predicts a longer time to failure for thicker nanowires than thinner ones, consistent with our experimental observations. The measured time to failure of nanowires under cyclic loading conditions can also be explained in terms of this mechanism.**

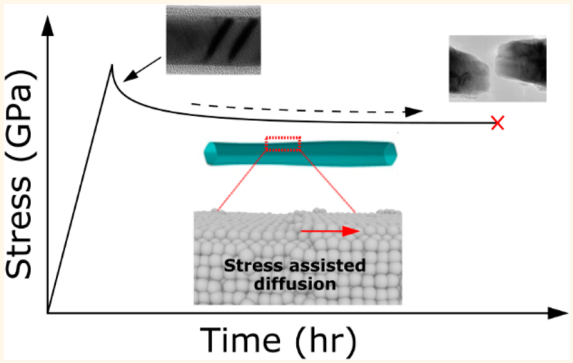


**KEYWORDS:** *nanowires, single crystal, stress-relaxation, flexible electronics, reliability, failure, fatigue*

Thin films of conductive, transparent, and flexible electrodes form a vital part of touch screens, solar panels, flexible electronics, and e-readers/papers. The most common material used for such electrodes in the industry is indium tin oxide (ITO) but recently ITO is getting replaced by metallic nanowires, such as silver and copper, given their low cost and superior electrical properties.[1,2] Given these wide range of uses for electrodes fabricated using nanowires, their mechanical and electromechanical properties must be characterized in order to understand their reliability and robustness in such applications. A plethora of work has been conducted recently on the mechanical and electromechanical properties at the macroscale composite level on the flexible polymer–nanowire films. Specifically, they have been characterized extensively in cyclic loading conditions. Many of these studies conclude that the electrical resistivity of flexible films increases with time and after many cyclic loadings of the flexible film.[3−7] The reason for such increase in electrical resistivity has been attributed to a variety of possibilities in the literature such as fatigue of the flexible substrate, electromigration, delamination of the nanowires from the flexible substrate and nanowire failure due to Joule heating. In order to understand the time-dependent properties of these flexible composite films, a systematic study of the time-dependent response of its key conducting component, the nanowires, needs to be conducted. Such study is now possible due to advances in the mechanical characterization of one-dimensional nanomaterials, such as nanowires, nanotubes, nanopillars, etc. *In situ* SEM and TEM nanomechanical testing using micro electromechanical systems

Received: February 15, 2017
Accepted: April 24, 2017
Published: April 24, 2017



DOI: 10.1021/acsnano.7b01075
ACS Nano 2017, 11, 4768−4776

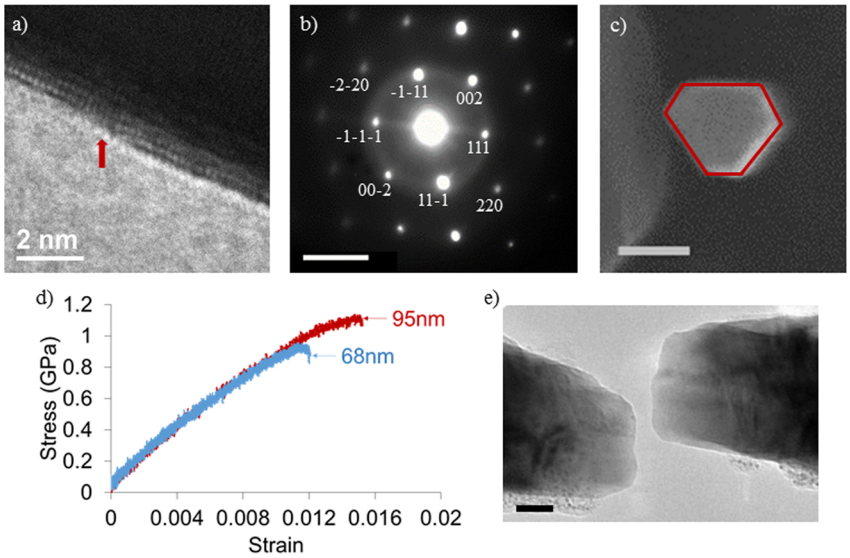


**Figure 1. (a) HRTEM image of a single crystalline silver nanowire surface with minor surface/step defects. (b) Indexed SAED image (scale bar is 5 nm$^{-1}$) with a zone axis of [1$\bar{1}$1] and the growth axis of [110]. (c) SEM image of the nanowire cross-section (scale bar: 100 nm). (d) Monotonic loading curves of single crystal silver nanowires under displacement control. (e) Fracture region of the nanowire imaged using HRTEM at high magnification (scale bar: 20 nm).**

(MEMS)-based platforms are currently being pursued at several laboratories around the world.[8] Previous research on metallic nanowires have reported extra-ordinary mechanical[9−11] and electromechanical properties.[1] For the most part, the metallic nanowires have been tested only in load control under monotonic loading conditions, at quasi-static[11−13] and high strain rates.[9] Due to the experimental complexity, only a few nanowire tests have been conducted under displacement control.[10,14]

There have been several reports on the size-dependent mechanical properties of nanowires, while only a very few studies have been reported on their time-dependent mechanical behavior. One of the reasons for the lack of time-dependent nanomechanical tests is the requirement to have stable MEMS-based testing platforms capable of outputting electrical signals without significant time-dependent drift.[15,16] Traditionally, time-dependent anelastic properties of materials are assessed via creep experiments, where the specimen is allowed to undergo deformation under a constant load or stress, or via stress-relaxation experiments, where the strain is held constant and the load is allowed to vary.[17] Thus, in order to properly assess the anelastic behavior of materials, the nanomechanical testing platforms should have the capability to conduct true force and displacement control capabilities, respectively. This is typically achieved using real-time fast-response feedback control to keep the force or displacement constant for the duration of the test. However, in the few recent studies conducted on the time-dependent properties of nanomaterials, such as the viscoplastic properties of gold thin films[18] and the recoverable plasticity of penta-twinned silver nanowires,[19] the employed MEMS-based testing platforms have been incapable of maintaining a constant stress or strain during the test. Thus, extraction of important nanomaterial properties, such as creep, creep-rupture, and stress-relaxation, have proven difficult.[20]

In this work, we report *in situ* SEM and TEM tests of single crystal silver nanowires under monotonic loading, cyclic loading, and stress-relaxation conditions, conducted using a MEMS-based testing platform capable of characterizing the mechanical response of nanomaterials under displacement control. During *in situ* SEM tests where the nanowires were held at a constant strain of 1%, stress-relaxation was initially observed, followed by a remarkable time-dependent rupture. Subsequent *in situ* TEM studies and molecular dynamics (MD) simulations conducted to understand the deformation mechanisms responsible for the observed stress-relaxation, revealed the formation of a few dislocations and stacking faults during the stress-relaxation time period. The initial stress-relaxation period only lasts for less than an hour, after which the stress remains constant for several hours, until the nanowires suddenly rupture. We hypothesize that the sudden rupture is caused by the stress-assisted diffusion, due to the amplification of surface perturbations at long wavelengths. This hypothesis is confirmed by our phase-field simulations. During tension−tension cyclic loading of nanowires, held at a mean strain of 1% and cycled with different strain amplitudes, we again found that the nanowire ruptures after a certain time period. The time to nanowire rupture for these cyclically loaded nanowires remained approximately the same as the nanowires tested under stress-relaxation conditions. This implied that even under cyclic loading, the time for nanowire rupture is controlled by the time for surface diffusion, rather than damage associated with the strain amplitude as in traditional fatigue mechanisms.

## RESULTS/DISCUSSION

**Displacement Control Tensile Testing under Monotonic Loading Conditions.** The structure of tested single crystal silver nanowires was characterized using bright field high-resolution TEM (HRTEM) imaging and diffraction pattern indexing as shown in Figure 1a,b. The single crystal silver nanowires were found to have a ⟨110⟩ growth direction and an approximately uniform cross-section over its length, expect for minor surface steps/defects, like the one pointed out in Figure 1a. By using SEM images of the ends of nanowires, grown perpendicular to the substrate, the cross-sectional morphology of the nanowires was identified as distorted hexagons as shown in Figure 1c.


DOI: 10.1021/acsnano.7b01075
ACS Nano 2017, 11, 4768−4776

Previous tensile testing results reported on nanowires have been obtained under loading conditions that are neither strictly load controlled nor displacement controlled.[9,11,12,18] In this work, we use a recently developed low-noise, high-resolution MEMS-based testing system capable of testing nanowires in displacement control.[14] This testing device uses a thermal actuator with chevron shaped beams, which when subjected to a particular input voltage displaces the shuttle where one end of the nanowire is mounted. The other end of the nanowire is mounted on a flexible load sensing shuttle. The shuttle is kept stationary during the tensile test by means of a feedback control loop consisting of a proportional-integral-derivative (PID) controller-based feedback loop and electrostatic actuation. Thus, the displacement applied by the thermal actuator equals the displacement of the nanowire and the load applied on the nanowire can be obtained from the electrostatic force applied using the actuation fingers. A brief description and working of this tensile testing device under displacement control is given in the Methods/Experimental Section and a more detailed description is provided elsewhere.[10,14] It should be noted that the projected width of the nanowires were measured from the SEM/TEM images, as shown in Figure S6. Given that we do not have the capability to rotate the nanowires, this width was used as the diameter of the circumcircle around the distorted hexagonal shape of the nanowire. As such, the cross-sectional area of this circumcircle was used to calculate the stress level in experiments.

Using this MEMS testing device, the single crystal silver nanowires were tested *in situ* SEM in monotonic loading conditions under displacement control. The stress−strain curves obtained for nanowires with different diameters are shown in Figure 1d. Given the lack of significant defects, such as twins/grain boundaries and the low strain rate of $10^{-4}$ $s^{-1}$ used for testing, the single crystal nanowires fail in a brittle-like fashion with very limited plasticity.[9] In order to understand the atomistic mechanisms involved in the failure process, a separate *in situ* TEM experiment was conducted. During the test, the nanowire remains defect free during the entire loading process and at approximately 1.3% strain the nanowire begins to develop a neck, most likely initiated through a defect on the nanowire surface. On further loading, the neck shrinks and the nanowire fails quickly in a highly localized unzipping-like manner (see Video 1 and Figure S2). The initial slip most likely localizes to a single crystal plane, as there are no other defect structures in the vicinity that can promote stabilized plasticity in the nanowires. The fracture surfaces of the nanowire imaged at high magnification using HRTEM are shown in Figure 1e.

**Displacement Control Tensile Testing under Stress-Relaxation Conditions.** The stress-relaxation tests were conducted using the MEMS device under displacement control. Since stress-relaxation tests typically involve testing periods over several hours, any potential time-dependent drift of the different input/output signals of the MEMS device needed to be characterized. It was found that after thermal equilibration, the thermal actuator displacement could be held constant, with an almost negligible drift of 0.58 nm/h, by applying a constant voltage through an arbitrary waveform generator (Agilent 33250A). The stability of the feedback control signal, characterized from the PID control signal sent to the electrostatic actuator, was also assessed over ∼20 h and proved to be highly stable, with a minimal signal drift of 11 mV/h (see Section S1 and Figure S1).

Using the previously obtained stress−strain data from the nanowires tested in monotonic loading conditions as reference, the appropriate input voltage for the thermal actuator, to apply 1% strain to the nanowires during the stress-relaxation test, was identified. Thus, during the *in situ* SEM stress-relaxation tests, by applying the proper voltage profile to the thermal actuator, the nanowires were quasistatically loaded up to a strain of ∼1% and held at this strain during the course of the test using the hardware-based real-time feedback loop. Figure 2 shows a

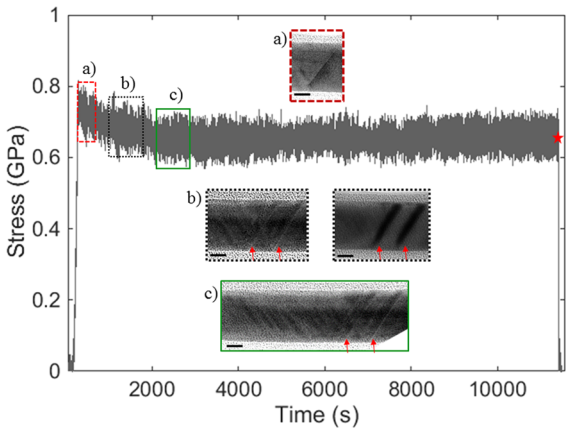


**Figure 2. *In situ* SEM stress-time curve of single crystal nanowire held at 1% strain exhibiting initial stress relaxation and final rupture after 3.5 h. Insets (a) HRTEM image of the nanowire showing that the initial stress relaxation arises from formation of a few stacking faults (SFs) in the nanowire. (b) and (c) As time increases, multiple slip bands appear close to the initial SFs as shown by the bright field and dark field images (scale bars: 20 nm).**

representative curve of the evolution of stress, as a nanowire with a diameter of 95 nm was held at a constant strain of 1%. As seen from Figure 2, in the initial stages of the test the stress relaxes by ∼135 MPa and beyond that the stress saturates to a constant value of ∼625 MPa. The relaxation time at constant strain was ∼2900 s. It should be noted that the peak-to-peak noise fluctuation in the stress level, determined by the standard deviation, during the stress-relaxation test is ∼34 MPa or the maximum fluctuation from the mean is 2.6%, as shown in Figure S7a).

Surprisingly, after continuing to hold the nanowire at the same strain of 1% for approximately 3.5 h, the nanowire ruptured abruptly, without any significant changes in the stress near the time of failure. This nanowire rupture after several hours into the test was indeed unexpected because the stress in the nanowire had already relaxed after 2900 s and has stayed at a constant value (lower than the initial stress) ever since. Further, under the same stress-relaxation conditions, a larger nanowire with a diameter of ∼110 nm was held at a constant strain of 1%. Similar to the smaller nanowire the stress in the nanowire relaxed and saturated initially, but the time to nanowire rupture had increased to ∼8.5 h. This observation strongly suggested alternative mechanisms of failure and warranted an in-depth study of the atomistic processes responsible for such unexpected material behavior.

**Atomistic Mechanisms—*In situ* TEM and MD Simulations.** In order to understand the atomistic mechanisms responsible for the stress-relaxation and the sudden rupture of the nanowires at a later time, we first used a combination of *in situ* TEM tests and MD simulations, which would allow the


DOI: 10.1021/acsnano.7b01075
ACS Nano 2017, 11, 4768−4776

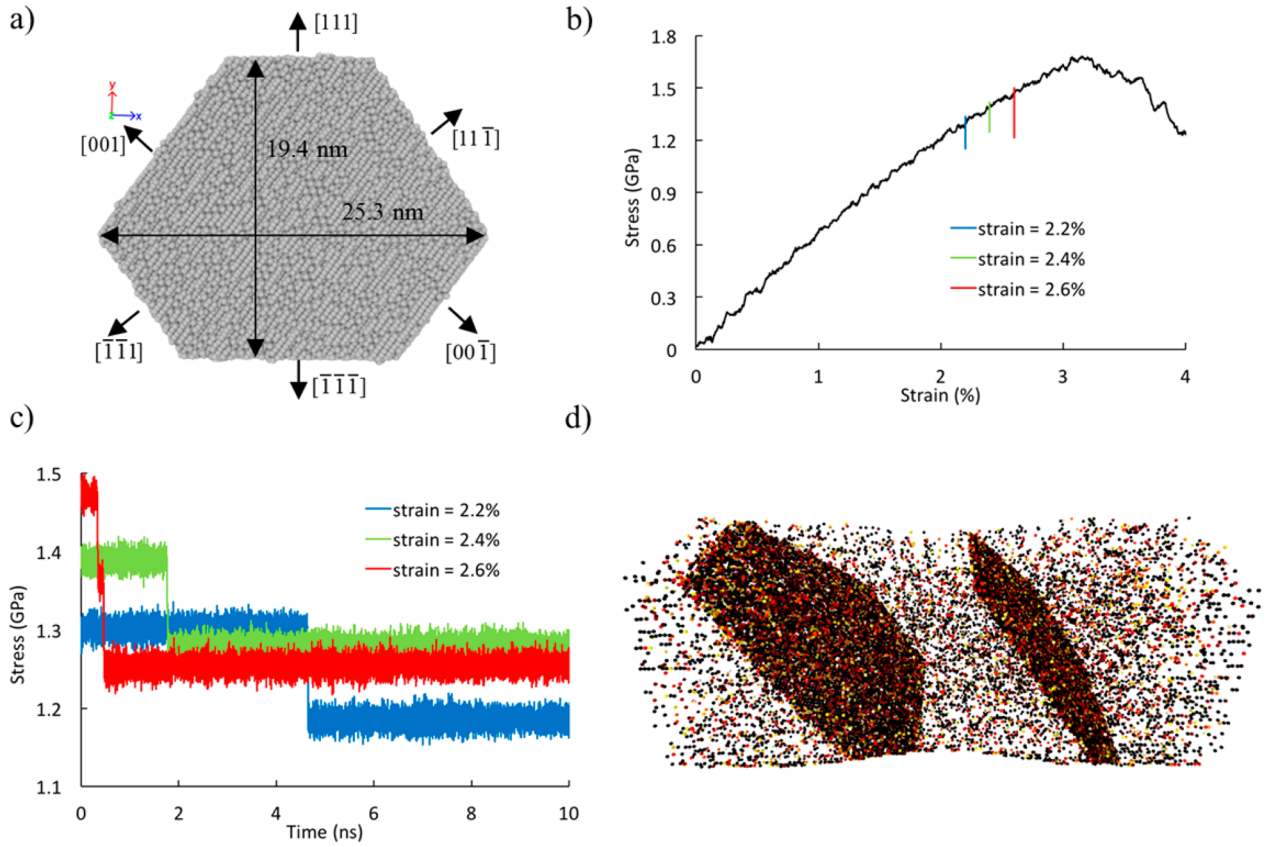


**Figure 3. (a) Cross section of the nanowire created for MD simulations. (b) Stress−strain curves of monotonic tensile tests and stress-relaxation tests conducted on the single crystalline nanowire with irregular hexagonal cross section using MD simulations. (c) Evolution of stress as a function of time during stress-relaxation tests conducted at different strain levels. (d) Two stacking faults are formed during the relaxation of the nanowire held at constant strain of 2.6%. For a clear representation, only the atoms with centrosymmetry parameter between 7 and 10 Å$^2$ are shown.**

observation of defect evolution as a function of time during the test. The *in situ* TEM stress-relaxation tests of nanowires held at a high strain revealed that during the initial part of the stress relaxation in the nanowire (less than 200 s) a fraction of the elastic strain in the nanowire was converted to plastic strain, leaving a few twins and stacking faults in the nanowire, as shown in Figure 2a.

Atomistic simulations were conducted to confirm the underlying mechanisms behind the stress-relaxation of the silver nanowires. A nanowire model, as shown in Figure 3a), was built using the information obtained from the experimental HRTEM, diffraction and SEM images as shown in Figures 1a−c. The details of the MD simulations are provided in the Methods/Experimental Section. The MD simulations revealed that when the nanowire is held at a constant strain of 2.6, 2.4, and 2.2% (close to but below the yield point in MD), the stress relaxes by ∼220, ∼100, and ∼100 MPa, respectively, as shown in Figure 3b,c. Similar to the experiments, the simulations confirm that the stress-relaxes in the nanowire by dislocation nucleation, leading to a few stacking faults and twins, as shown in Figure 3d. The authors acknowledge that there is a discrepancy between the strain value used to hold the nanowire between the experiments and simulations. In the experiments 1% strain was chosen as a value close to the yield strain of 1.3% found from monotonic loading experiments. On the other hand, in MD simulations owing to the much higher strain rate compared to experiments, upon monotonic loading, the yield strain obtained was approximately 3.2%. Thus, in order to stay close to the yield point, the stress-relaxation MD simulations were conducted at 2.6, 2.4, and 2.2% strains. The limited simulation time period of 10 ns was fortunately sufficient to capture the atomistic mechanisms behind the stress-relaxation phenomena. Thus, both HRTEM observations and MD simulations indicate that the mechanism of stress relaxation in single crystal silver nanowires is dislocation nucleation.

Beyond the initial relaxation time period (i.e., from 200 to 2900 s), the stress in the nanowire relaxes further by virtue of slip bands near the vicinity of the initial twins and stacking faults as shown by the bright field and dark field images in Figure 2b. A HRTEM snapshot of the propagated slip bands and other defects in the nanowire, just before the saturated stress level is achieved, is shown in Figure 2c. Surprisingly, once the stress saturates in the nanowire and until it abruptly ruptures at ∼3.5 h, there were no significant changes in the number of defects observed using sequential HRTEM imaging. It should be noted that in order to avoid the electron beam damage of the nanowire, the nanowire was imaged at sequential time intervals of 15 min and the electron beam was turned off in between the images. Since the rupture of the nanowire happened abruptly at ∼3.5 h, it could not be captured by the TEM images, but the images of the nanowire post failure are shown in Section S2. By simply comparing the nanowire failed under monotonic loading and stress-relaxation conditions, as shown in Section S2, it is clear that the mechanisms involved in the failure of nanowires in these two cases are different. The nanowire tested at monotonic loading condition, fails by


DOI: 10.1021/acsnano.7b01075
ACS Nano 2017, 11, 4768−4776

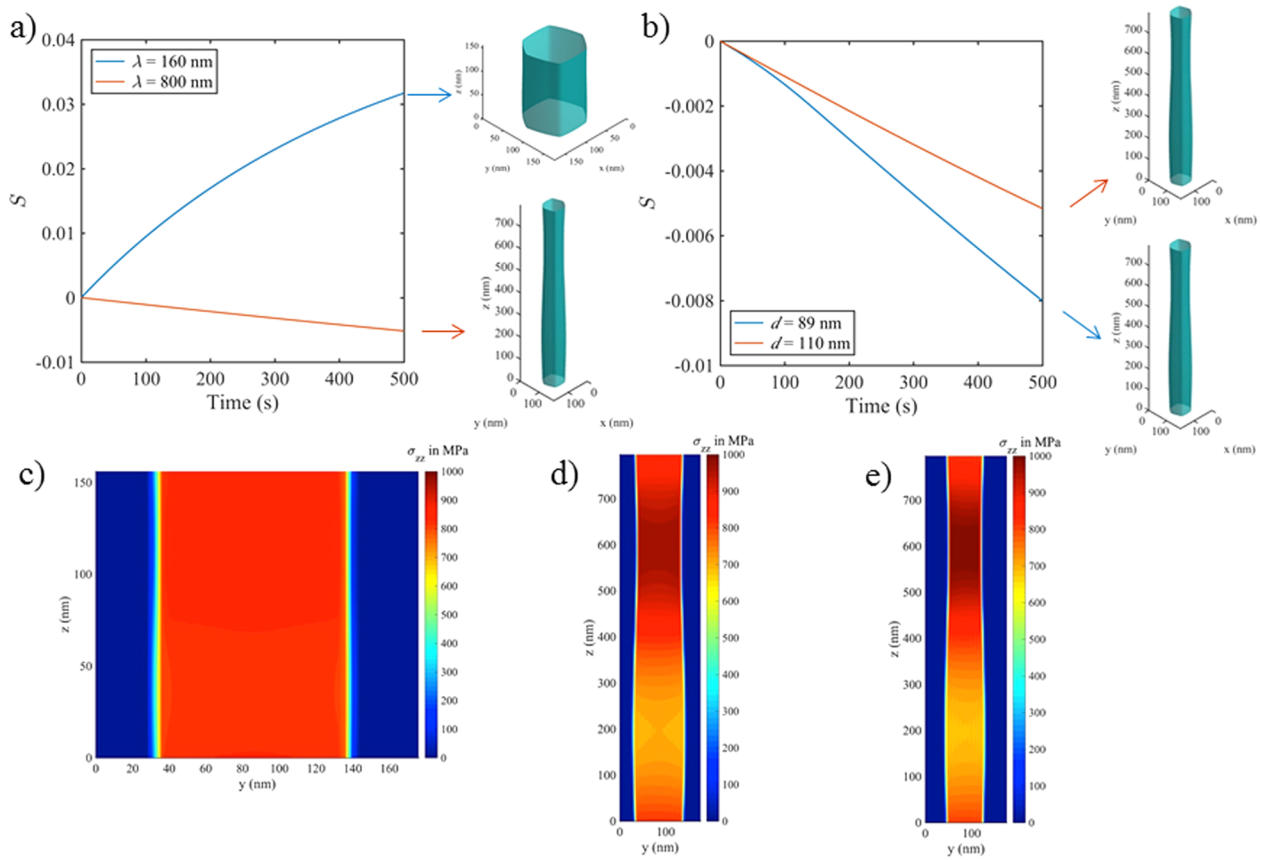


**Figure 4. (a) Cross section area change as a function of time at different initial perturbation wavelengths given the same nanowire diameter of 110 nm. (b) Cross section area change as a function of time for different nanowire diameters given the same initial perturbation wavelength of 800 nm. Longitudinal section view of the tensile stress $\sigma_{zz}$ distribution of nanowires at (c) $d$ of 110 nm and $\lambda$ of 160 nm (left), (d) $d$ of 110 nm and $\lambda$ of 800 nm (middle), and (e) $d$ of 89 nm and $\lambda$ of 800 nm (right).**

localized plasticity in one small region in the nanowire and the rest of the wire remains defect free. On the other hand, the nanowire ruptured under stress-relaxation conditions show two to four necking regions along the length of the nanowire. Given the unpredictable sudden rupture of the nanowire after holding it at a high strain for several hours, the responsible atomistic mechanisms for the failure could not be identified using either *in situ* TEM characterizations or MD simulations.

**Phase Field Modeling and Analytical Analysis.** We hypothesize that the nanowire failure under the stress-relaxation condition is caused by stress-induced surface roughening via diffusion.[21,22] The roughening of the nanowire surface can reduce the total elastic energy, but it also changes the cross sectional area of the wire. This results in the stress concentration at the thinner regions, which ultimately leads to the final rupture. To verify this hypothesis, we developed a phase field model that accounts for the elastic energy (the detailed formulation of the model is provided in Section S3). Given that initially the nanowire surface is not perfectly smooth, as shown from the HRTEM image in Figure 1a, we approximated the initial shape of the nanowire by adding a sinusoidal function (with a small amplitude and a wavelength $\lambda$) to the average diameter $d$. The phase field simulations were performed with different average nanowire diameter $d$ and surface perturbation wavelength $\lambda$. Under the same 1% strain, the changes in nanowire cross sectional area were monitored, in order to quantify the different behaviors of the wire with different $d$ or $\lambda$.

Here we define the relative change of the cross section area as $S = (A^t_{\min} - A^0_{\min})/A^0_{\min}$, where $A^0_{\min}$ is the minimum cross section area at the beginning of the simulation, and $A^t_{\min}$ is the cross section area at the same necking region at time $t$. Figure 4a shows that for the same $d$, when $\lambda$ is small, the nanowire starts to recover from the perturbed shape ($S$ increasing with time). Because diffusion conserves the total volume of the nanowire, this recovery results in the expansion at the necking region and the shrinkage at the bulging region, before reaching the equilibrium where the diameter becomes completely uniform along the nanowire. The nanowire with the same $d$ but larger $\lambda$ experiences an amplification of the surface perturbation ($S$ decreasing with time). Figure 4b shows that for the same $\lambda$, the nanowire with smaller $d$ experiences a more rapid growth of the instability ($S$ decreasing faster with time).

Figure 4c, d, and e provide the longitudinal section view of the $\sigma_{zz}$ stress distribution of nanowires at the end of three different simulations conducted with varying $\lambda$ and $d$. In Figure 4c, when $\lambda$ is small enough, the $\sigma_{zz}$ is distributed almost uniformly along the $z$ direction. Both Figure 4d and Figure 4e observe higher stress at the thinner region of the wire. The calculations show that the maximum stress for the nanowire with $d$ = 89 nm is 1000 MPa, which is higher than 950 MPa for nanowire with $d$ = 110 nm. This indicates that given the same strain for the same time period, a thinner nanowire experiences a higher local stress, which eventually leads to earlier nanowire rupture. It can be noticed in Figure 4d and Figure 4e that the nanowire surface morphology change needed for creating such


DOI: 10.1021/acsnano.7b01075
ACS Nano 2017, 11, 4768−4776

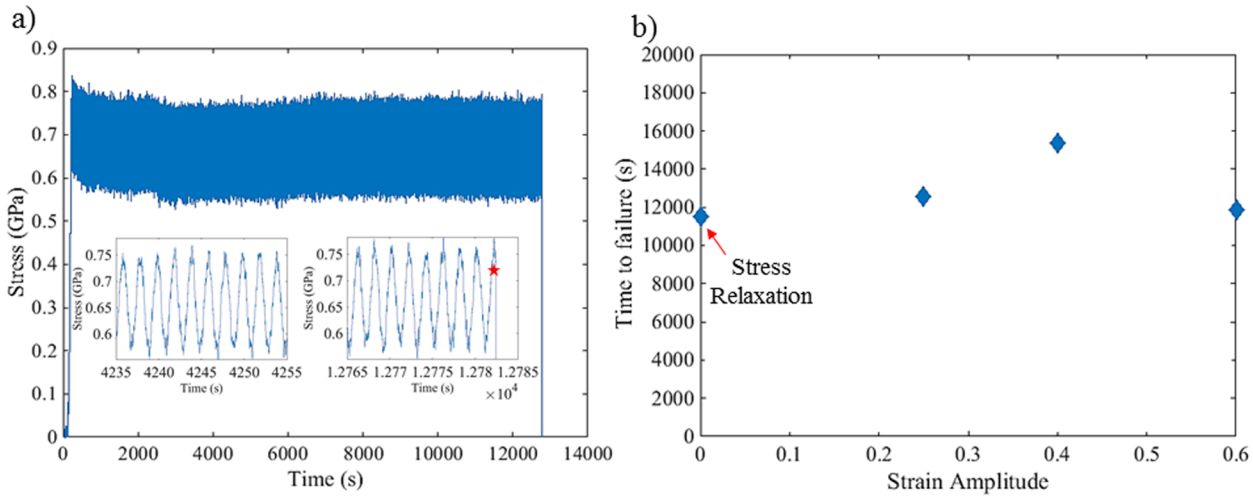


**Figure 5. Cyclic loading of nanowires. (a) Stress-time curve of a single crystal silver nanowire held at 1% strain and cycled with a strain amplitude of 0.25%. (b) Summary of cyclically loaded nanowire time to failure at different strain amplitudes with a mean strain of 1%.**

high internal stress differences (~150 MPa) is on the order of 5 nm, smoothly distributed over a length of hundreds of nanometers. Such small changes of the surface morphology are very difficult to observe in TEM, especially when the nanowire is intentionally imaged at low magnifications of 8000× to avoid beam damage. This type of change in surface morphology due to stress-assisted diffusion has been previously observed in heteroepitaxial thin films.[23,24] In experiments, as shown in Figure 2, the global stress levels in the nanowire remain constant beyond the initial stress-relaxation until failure. On the other hand, phase field simulations show that the nanowire develops stress concentrations due to stress-assisted diffusion and the evolution of the maximum local stresses with time as shown in Figure S5. It can be seen clearly that the maximum local stresses keep rising with time, which eventually leads to nanowire failure, though this increasing localized stress is not reflected in the global stress recorded in experiments.

From the competition between the elastic energy change and the surface energy change, analytical solutions have been proposed and widely accepted, for explaining the surface roughening of epitaxial thin films on an elastic half space induced by stress.[23,25] Following the same steps, we derived an analytical expression for the stress-induced surface roughening of nanowire, in order to better understand the mechanisms of nanowire failure and justify our phase field simulations. Specifically, we predicted a critical strain $\varepsilon_c$ above which the surface perturbation will become larger with time, as shown by eq 1 (for a detailed derivation of this analytical model, please see Section S5)

$$\varepsilon_c = \frac{2\pi}{\sqrt{3}\lambda}\sqrt{\frac{\gamma d}{E}} \tag{1}$$

where $d$ is the diameter of the nanowire, $\gamma$ is the surface energy, $E$ is the elastic modulus, and $\lambda$ is the wavelength of the surface perturbation. Eq 1 suggests that increasing $\lambda$ or decreasing $d$ reduces the surface stability, which indicates that at a given applied strain, the surfaces are easier to roughen, for thin nanowires and/or wires with long-wavelength surface perturbation. This is consistent with the predictions from the phase field modeling.

In addition, the critical strain $\varepsilon_c$ can be related to the required loading time $t$ for nanowire failure. Under this diffusion dominant process, the time to failure $t$ can be considered as the diffusion time that scales with $\lambda^2/D$, where $D$ is the diffusivity. Therefore, eq 1 can be rearranged to give,

$$t = \frac{4\pi^2\gamma d}{3ED\varepsilon^2} \tag{2}$$

For a nanowire of diameter 100 nm with a perturbation wavelength of 400 nm, the critical strain to failure is ~1%, which is similar to the strain used in the experiments. Choosing $\gamma = 1\ \mathrm{J/m^2}$, $E = 83$ GPa, and $D = 10^{-17}\ \mathrm{m^2/s}$ for silver, based on eq 2, the time to failure calculated for a nanowire of 100 nm diameter held at a strain of 1% is ~4.4 h, which is also a close match to the experiments.

Chen et al. recently suggested that at high stresses surface diffusion mechanism maybe responsible for dislocation formation in pristine palladium nanowires tested in monotonic loading conditions at a variety of temperatures.[11] Similarly, here we show that stress-assisted diffusion could also be responsible for nanowire rupture when the nanowire is held at a high strain for long periods of time.

**Displacement Control Tensile Testing under Cycling Loading Conditions.** As mentioned before, one emergent application for nanowires is in flexible electronics, where nanowires are subject to a variety of cyclic loading. So, the mechanical behavior of single crystal silver nanowires, subject to fatigue-like tension−tension cyclic loading was also investigated under displacement control using the same MEMS testing platform. Nanowires with a diameter of 95 nm were quasistatically loaded to the same mean strain of 1%, and then cyclically loaded between different strain amplitudes, ranging from 0.25 to 0.6%.

Similar to the behavior of the nanowires tested under stress-relaxation conditions, the stress in the nanowires relaxed and saturated during the course of the repeated cyclic loadings, as shown in Figure 5a. Again similar to the constant strain tests, the nanowire abruptly ruptures after being cyclically loaded for several hours. Several nanowires were tested at different strain amplitudes, as shown in Figure 5b, but surprisingly all the nanowires ruptured in approximately the same time taken by the nanowire under simple constant strain of 1%. Hence, these experimental results reveal that the time-dependent mechanical behavior of the nanowire is primarily controlled by the mean


DOI: 10.1021/acsnano.7b01075
ACS Nano 2017, 11, 4768−4776

strain and not by the cyclic loads. These tests further prove the point that surface diffusion driven by the reduction of elastic energy was indeed responsible for the failure of the nanowires.

## CONCLUSION

In summary, we have characterized the mechanical behavior of single crystal silver nanowires under stress-relaxation and cyclic loading conditions using *in situ* electron microscopy, atomistic simulations and phase-field modeling. Both the experiments and MD simulations show that the initial stress-relaxation in the nanowire is caused by dislocation nucleation. Using phase field and analytical modeling, it was shown that the final rupture of the nanowires is caused by surface instability due to stress-assisted diffusion.

These results obtained from the time-dependent testing of nanowires, could potentially have significant implications on many existing nanowire-based systems. For example, the time for nanowire rupture depends on the strain applied on the nanowire. This phenomenon could explain the increase in electrical resistance in touch screens, made of percolating networks of nanowires, after several days of usage, as reported in the literature.[4,7] It is possible that the nanowires in touch screen have a residual strain from the manufacturing process or from the application that could lead to the failure of nanowires, which in turn would result in an increase of electrical resistance in the screen. Similarly in flexible composites, where nanowires are subjected to repeated cyclic loads at different strains, the electrical resistivity of the films has been shown to increase after several cycles.[3] This can also be attributed to nanowire rupture triggered by surface instabilities due to cyclic loading. For example, Hwang et al. tested flexible films with silver nanowire networks under tension and compression bending cycles.[5] The HRTEM images of the nanowires reported by Hwang et al., after they have been through several cyclic loadings, show that many nanowires have indeed ruptured, with multiple necks along the length of the nanowire.[5] This failure mode is very similar to the HRTEM images of the failed individual nanowires, tested under both stress-relaxation and cyclic conditions as shown representatively in Section S2.

New research fields, such as ultrastrength materials and elastic strain engineered materials, critically depend on the time, temperature, and size effect of nanomaterials for applying large stresses without significant relaxation or time dependent failure. Relaxation of stress due to defect nucleation and further rupture due to stress-assisted diffusion as exhibited by the silver nanowires discussed above, can potentially degrade the functionality of many strain-engineered devices.[26] Thus, it is vital to identify nanomaterials that can sustain large tensile strains without significant inelastic relaxations by plasticity or fracture through suppressing dislocation nucleation.[27] This warrants further investigations on the time-dependent properties of other metallic nanowires, such as penta-twinned and core−shell nanowires.[7] Such studies could provide valuable information on the potential impact of the twin boundaries and the core−sheath radial boundaries on the time-dependent properties of the nanowires, especially the rupture after holding at high strains.

## METHODS/EXPERIMENTAL

The first step for testing of nanowires using the MEMS device involves the nanomanipulation and mounting of the nanowire across the thermal actuator and the load sensor shuttles using electron beam induced deposition (EBID) of platinum. A voltage is then applied to the thermal actuator chevron shaped beams, which displaces the beams and in turn moves the shuttle where one end of the nanowire is attached. Thus, the thermal actuator controls the strain applied to the nanowire. The nanowire is attached to the load sensor on the other side, where using interdigitated fingers a capacitance change is produced proportional to the displacement and converted to a voltage using a commercial capacitance sensing chip (MS3110). This voltage is compared to a reference that corresponds to the equilibrium position, i.e., with zero displacement and the error is inputted into a PID controller (Stanford Research Systems SIM960). The PID controller computes in real-time an actuation voltage to be applied to the electrostatic actuation fingers, in order to keep the load sensor stationary. Thus, the displacement of the nanowire equals the thermal actuator displacement and the electrostatic force applied by the actuation fingers equals the force applied on the nanowire.

The single crystal nanowires were synthesized by physical vapor deposition at 800 °C under ultrahigh vacuum conditions using molecular beam epitaxy method. A detailed description of this nanowire synthesis process is provided elsewhere.[13]

**MD Simulation.** MD simulations were conducted using the LAMMPS software package.[28] The EAM interatomic potential[29] was used to model the interactions between silver atoms. The nanowire has an irregular hexagonal cross section with a diameter of 22 nm and length of 39.3 nm. Periodic boundary condition is applied along the axis. In order to better mimic the experimental conditions, a surface roughness was included in the nanowire by randomly removing 80% of atoms on the outermost layer of atoms and 20% of the second layer. The nanowire contains 802,862 silver atoms. It is first relaxed for about 0.5 ns at an elevated temperature of 800 K with a time-step size of $10^{-15}$ s until the nanowire equilibrates and becomes stress-free along the axis. Nose−Hoover thermostat and barostat are used to maintain the temperature and pressure of the system. The stress is computed by the Virial stress expression, which corresponds to the average stress over the entire nanowire. We then stretch the nanowire with a strain rate of $10^8$ $s^{-1}$ at the same temperature. After reaching a certain level of elastic strain, the stretching is stopped and the nanowire is relaxed for 2 ns. The elevated temperature helps us to accelerate thermally activated processes, such as dislocation nucleation and surface diffusion, which are crucial for observing the relaxation process within the MD time scale. Stacking faults and twin boundaries were identified using OVITO.[30]

**Phase Field Simulation.** Three independent phase field simulations are performed for studying the stress-induced nanowire surface roughening.[31,32] The detailed formulation of the model is discussed in Section S3, with the key parameters of the model provided in Section S4. For all three simulations, 1% tensile strain is applied along the nanowire axial [110] direction. Keeping the elastic properties and the interfacial energy the same, for Case 1, the nanowire diameter $d$ is set to 110 nm and the initial perturbation wavelength $\lambda$ is set to 160 nm, which corresponds to a critical strain $\varepsilon_c$ larger than 1%, according to eq 1. For Case 2, $d$ is kept at 110 nm, but $\lambda$ is extended to 800 nm. For Case 3, $\lambda$ is kept at 800 nm, but $d$ is reduced to 89 nm. A $10^5$-step phase field simulation is run for each condition with a time step of 5 ms. Within each time step, the elastic field is evolved for 10 subcycles to solve for the elastic energy distribution for the given phase field.

## ASSOCIATED CONTENT

### Supporting Information

The Supporting Information is available free of charge on the ACS Publications website at DOI: 10.1021/acsnano.7b01075.

Experimental methodology of MEMS-based displacement controlled tensile testing with active feedback control and the stability of the electrical signals, comparison between the post-mortem HRTEM images of nanowires failed under monotonic loading and stress-relaxation conditions, methodology behind phase field modeling of the nanowire, parameters chosen for the



DOI: 10.1021/acsnano.7b01075
ACS Nano 2017, 11, 4768−4776

phase field model, and derivation of the analytical solution used to identify the critical strain needed for nanowire surface roughening (PDF)

Supplementary Video 1 showing the nanowire monotonically loaded under displacement control, the nanowire fails in a localized unzipping-like manner (AVI)

## AUTHOR INFORMATION


### Corresponding Authors

*espinosa@northwestern.edu.

*caiwei@stanford.edu.

### ORCID

Yanming Wang: 0000-0002-0912-681X

Horacio D. Espinosa: 0000-0002-1907-3213


### Author Contributions

⊥R.R. performed and analyzed the experiments. Y.W. performed the phase field modeling and analytical analysis. A.A. conducted the atomistic simulations. G.R. synthesized the single crystal silver nanowires used in the experiments. H.D.E. and W.C. conceived the research and provided guidance throughout the research. All authors discussed the results, cowrote, and commented on the manuscript. R.R. and Y.W. contributed equally.

### Notes

The authors declare no competing financial interest.

## ACKNOWLEDGMENTS

H.D. Espinosa gratefully acknowledges support from NSF through award No. DMR-1408901. We thank Dr. F. Shi for help with TEM imaging. This work made use of the EPIC, Keck-II, and/or SPID facility(ies) of Northwestern University's NUANCE Center, which has received support from the Soft and Hybrid Nanotechnology Experimental (SHyNE) Resource (NSF NNCI-1542205); the MRSEC program (NSF DMR-1121262) at the Materials Research Center; the International Institute for Nanotechnology (IIN); the Keck Foundation; and the State of Illinois, through the IIN.

## REFERENCES


(1) Bernal, R. A.; Filleter, T.; Connell, J. G.; Sohn, K.; Huang, J.; Lauhon, L. J.; Espinosa, H. D. *In Situ* Electron Microscopy Four-Point Electromechanical Characterization of Freestanding Metallic and Semiconducting Nanowires. *Small* **2014**, *10*, 725−733.

(2) Langley, D.; Giusti, G.; Mayousse, C.; Celle, C.; Bellet, D.; Simonato, J.-P. Flexible Transparent Conductive Materials Based on Silver Nanowire Networks: A Review. *Nanotechnology* **2013**, *24*, 452001.

(3) Amjadi, M.; Pichitpajongkit, A.; Lee, S.; Ryu, S.; Park, I. Highly Stretchable and Sensitive Strain Sensor Based on Silver Nanowire−Elastomer Nanocomposite. *ACS Nano* **2014**, *8*, 5154−5163.

(4) Khaligh, H. H.; Goldthorpe, I. A. Failure of Silver Nanowire Transparent Electrodes under Current Flow. *Nanoscale Res. Lett.* **2013**, *8*, 235.

(5) Hwang, B.; Kim, T.; Han, S. M. Compression and Tension Bending Fatigue Behavior of Ag Nanowire Network. *Extreme Mechanics Letters* **2016**, *8*, 266−272.

(6) Ko, Y.; Song, S. K.; Kim, N. H.; Chang, S. T. Highly Transparent and Stretchable Conductors Based on a Directional Arrangement of Silver Nanowires by a Microliter-Scale Solution Process. *Langmuir* **2016**, *32*, 366−373.

(7) Rathmell, A. R.; Nguyen, M.; Chi, M.; Wiley, B. J. Synthesis of Oxidation-Resistant Cupronickel Nanowires for Transparent Conducting Nanowire Networks. *Nano Lett.* **2012**, *12*, 3193−3199.

(8) Ramachandramoorthy, R.; Bernal, R.; Espinosa, H. D. Pushing the Envelope of *in Situ* Transmission Electron Microscopy. *ACS Nano* **2015**, *9*, 4675−4685.

(9) Ramachandramoorthy, R.; Gao, W.; Bernal, R.; Espinosa, H. High Strain Rate Tensile Testing of Silver Nanowires: Rate-Dependent Brittle-to-Ductile Transition. *Nano Lett.* **2016**, *16*, 255−263.

(10) Bernal, R. A.; Aghaei, A.; Lee, S.; Ryu, S.; Sohn, K.; Huang, J.; Cai, W.; Espinosa, H. Intrinsic Bauschinger Effect and Recoverable Plasticity in Pentatwinned Silver Nanowires Tested in Tension. *Nano Lett.* **2015**, *15*, 139−146.

(11) Chen, L. Y.; He, M.-r.; Shin, J.; Richter, G.; Gianola, D. S. Measuring Surface Dislocation Nucleation in Defect-Scarce Nanostructures. *Nat. Mater.* **2015**, *14*, 707−713.

(12) Filleter, T.; Ryu, S.; Kang, K.; Yin, J.; Bernal, R. A.; Sohn, K.; Li, S.; Huang, J.; Cai, W.; Espinosa, H. D. Nucleation-Controlled Distributed Plasticity in Penta-Twinned Silver Nanowires. *Small* **2012**, *8*, 2986−2993.

(13) Richter, G.; Hillerich, K.; Gianola, D. S.; Monig, R.; Kraft, O.; Volkert, C. A. Ultrahigh Strength Single Crystalline Nanowhiskers Grown by Physical Vapor Deposition. *Nano Lett.* **2009**, *9*, 3048−3052.

(14) Pantano, M. F.; Bernal, R. A.; Pagnotta, L.; Espinosa, H. D. Multiphysics Design and Implementation of a Microsystem for Displacement-Controlled Tensile Testing of Nanomaterials. *Meccanica* **2015**, *50*, 549−560.

(15) Gupta, S.; Pierron, O. N. Mems Based Nanomechanical Testing Method with Independent Electronic Sensing of Stress and Strain. *Extreme Mechanics Letters* **2016**, *8*, 167−176.

(16) Cheng, G.; Miao, C.; Qin, Q.; Li, J.; Xu, F.; Haftbaradaran, H.; Dickey, E. C.; Gao, H.; Zhu, Y. Large Anelasticity and Associated Energy Dissipation in Single-Crystalline Nanowires. *Nat. Nanotechnol.* **2015**, *10*, 687−691.

(17) Nowick, A. S. *Anelastic Relaxation in Crystalline Solids* **1972**, *1*, 3−9.

(18) Qin, Q.; Yin, S.; Cheng, G.; Li, X.; Chang, T.-H.; Richter, G.; Zhu, Y.; Gao, H. Recoverable Plasticity in Penta-Twinned Metallic Nanowires Governed by Dislocation Nucleation and Retraction. *Nat. Commun.* **2015**, *6*, 5983.

(19) Hosseinian, E.; Legros, M.; Pierron, O. N. Quantifying and Observing Viscoplasticity at the Nanoscale: Highly Localized Deformation Mechanisms in Ultrathin Nanocrystalline Gold Films. *Nanoscale* **2016**, *8*, 9234−9244.

(20) Mohanty, G.; Wehrs, J.; Boyce, B. L.; Taylor, A.; Hasegawa, M.; Philippe, L.; Michler, J. Room Temperature Stress Relaxation in Nanocrystalline Ni Measured by Micropillar Compression and Miniature Tension. *J. Mater. Res.* **2016**, *31*, 1085.

(21) Goldthorpe, I. A.; Marshall, A. F.; McIntyre, P. C. Inhibiting Strain-Induced Surface Roughening: Dislocation-Free Ge/Si and Ge/Sige Core− Shell Nanowires. *Nano Lett.* **2009**, *9*, 3715−3719.

(22) Wang, Y. U.; Jin, Y. M.; Khachaturyan, A. G. Phase Field Microelasticity Theory and Modeling of Elastically and Structurally Inhomogeneous Solid. *J. Appl. Phys.* **2002**, *92*, 1351−1360.

(23) Freund, L. B.; Suresh, S. *Thin Film Materials: Stress, Defect Formation and Surface Evolution*; Cambridge University Press, 2004; pp 615−618.

(24) Gao, H. Some General Properties of Stress-Driven Surface Evolution in a Heteroepitaxial Thin Film Structure. *J. Mech. Phys. Solids* **1994**, *42*, 741−772.

(25) Gao, H.; Nix, W. D. Surface Roughening of Heteroepitaxial Thin Films. *Annu. Rev. Mater. Sci.* **1999**, *29*, 173−209.

(26) Li, J. Dislocation Nucleation: Diffusive Origins. *Nat. Mater.* **2015**, *14*, 656−657.

(27) Li, J.; Shan, Z.; Ma, E. Elastic Strain Engineering for Unprecedented Materials Properties. *MRS Bull.* **2014**, *39*, 108−114.

(28) Plimpton, S. Fast Parallel Algorithms for Short-Range Molecular Dynamics. *J. Comput. Phys.* **1995**, *117*, 1−19.

(29) Williams, P.; Mishin, Y.; Hamilton, J. An Embedded-Atom Potential for the Cu−Ag System. *Modell. Simul. Mater. Sci. Eng.* **2006**, *14*, 817.




DOI: 10.1021/acsnano.7b01075
ACS Nano 2017, 11, 4768−4776

(30) Stukowski, A. Visualization and Analysis of Atomistic Simulation Data with Ovito–the Open Visualization Tool. *Modell. Simul. Mater. Sci. Eng.* **2010**, *18*, 015012.
(31) Wang, Y.; Ryu, S.; McIntyre, P. C.; Cai, W. A Three-Dimensional Phase Field Model for Nanowire Growth by the Vapor–Liquid–Solid Mechanism. *Modell. Simul. Mater. Sci. Eng.* **2014**, *22*, 055005.
(32) Wang, Y.; McIntyre, P. C.; Cai, W. Phase Field Model for Morphological Transition in Nanowire Vapor-Liquid-Solid Growth. *Cryst. Growth Des.* **2017**, *17*, 2211.



DOI: 10.1021/acsnano.7b01075
*ACS Nano* 2017, 11, 4768–4776